

LETTER • OPEN ACCESS

Soil cation storage is a key control on the carbon removal dynamics of enhanced weathering

To cite this article: Y Kanzaki *et al* 2025 *Environ. Res. Lett.* **20** 074055

View the [article online](#) for updates and enhancements.

You may also like

- [Forest dynamics mapping in central Vietnam from 1988 to 2022 using Landsat time-series data](#)
Hien Nguyen, Eike Behre, Hoang Khanh Linh Nguyen et al.
- [A review of methane emissions source types, characteristics, rates, and mitigation effectiveness across U.S. and Canadian cities](#)
Coleman Vollrath, Zhenyu Xing, Chris H Hugenholtz et al.
- [Multicore structures of oceanic mesoscale eddies](#)
Yanjiang Lin

UNITED THROUGH SCIENCE & TECHNOLOGY

ECS The Electrochemical Society
Advancing solid state & electrochemical science & technology

**248th
ECS Meeting**
Chicago, IL
October 12-16, 2025
Hilton Chicago

**Science +
Technology +
YOU!**

Register by
September 22
to save \$\$

REGISTER NOW

ENVIRONMENTAL RESEARCH
LETTERS

LETTER

Soil cation storage is a key control on the carbon removal dynamics of enhanced weathering

OPEN ACCESS

RECEIVED
31 January 2025REVISED
6 May 2025ACCEPTED FOR PUBLICATION
4 June 2025PUBLISHED
18 June 2025

Original content from this work may be used under the terms of the [Creative Commons Attribution 4.0 licence](#).

Any further distribution of this work must maintain attribution to the author(s) and the title of the work, journal citation and DOI.

Y Kanzaki^{1,*} , N J Planavsky^{2,3} , S Zhang⁴ , J Jordan⁵, T J Suhrhoff^{2,3} and C T Reinhard^{1,*} ¹ School of Earth and Atmospheric Sciences, Georgia Institute of Technology, Atlanta, GA, United States of America² Department of Earth and Planetary Sciences, Yale University, New Haven, CT, United States of America³ Yale Center for Natural Carbon Capture, New Haven, CT, United States of America⁴ Department of Oceanography, Texas A&M University, College Station, TX, United States of America⁵ Mati Carbon, Houston, TX, United States of America

* Authors to whom any correspondence should be addressed.

E-mail: ykanzaki3@gatech.edu and chris.reinhard@eas.gatech.edu**Keywords:** climate mitigation, carbon removal, agricultural greenhouse gas emissions, soil management, enhanced weatheringSupplementary material for this article is available [online](#)**Abstract**

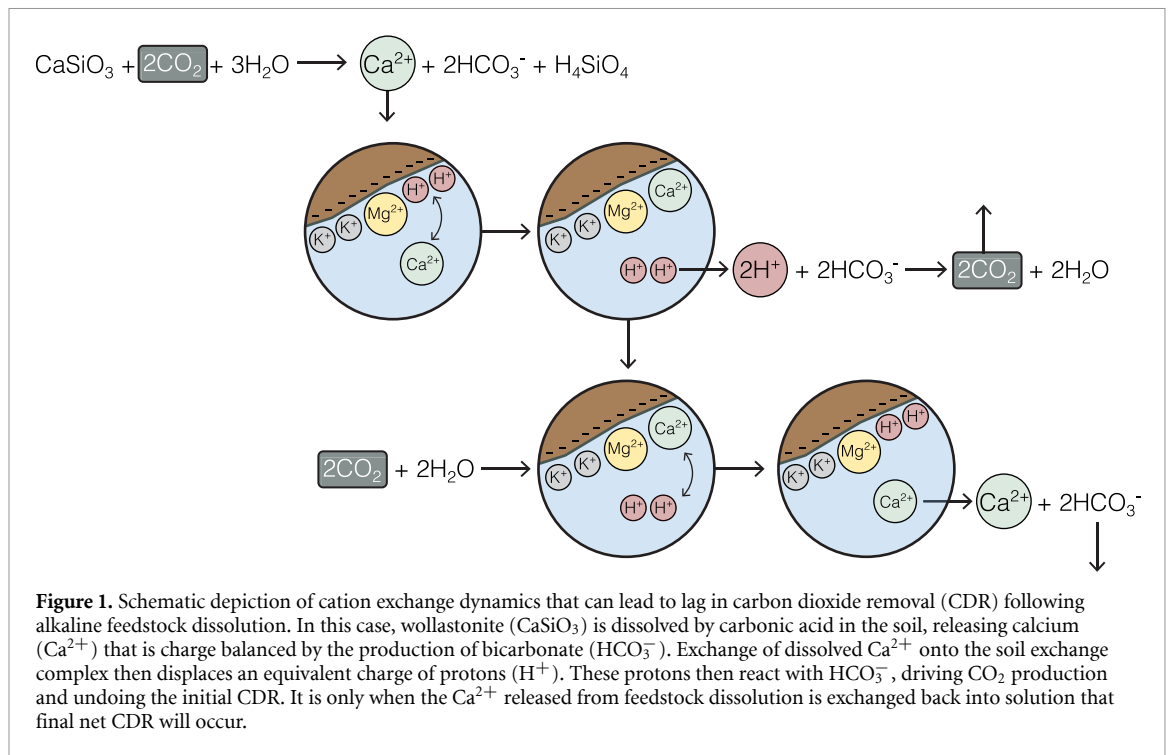
Significant interest and resources are currently being channeled into techniques for durable carbon dioxide removal (CDR) from Earth's atmosphere. A particular class of these approaches—referred to as enhanced weathering (EW)—seeks to modify the surface alkalinity budget to store CO₂ as dissolved inorganic carbon species. Here, we use a reaction-transport model designed to simulate EW in managed lands to evaluate the throughput and storage timescales of anthropogenic alkalinity in agricultural soils in the coterminous U.S. We find that lag times between alkalinity modification and carbon removal can span from years to many decades depending on region. Background soil cation exchange capacity, agronomic target pH, and fluid infiltration all impact the timescales of CDR relative to the timing of alkalinity input, suggesting there is scope for optimization of alkalinity transport through variation in land management practice. However, shifting practices to reduce lag times may decrease total CDR from weathering and lead to non-optimal nutrient use efficiencies and soil nitrous oxide (N₂O) fluxes. Our results indicate that there may be a large temporal disconnect between deployment of EW and climate-relevant CDR, with important implications for monitoring, reporting, and verifying carbon removal through EW.

1. Introduction

Efforts to limit the extent of future anthropogenic climate disruption will likely require significant amounts of net carbon dioxide removal (CDR) from Earth's atmosphere. Even optimistic scenarios for decarbonization of energy systems, transport, and industry in the coming decades still require roughly 1–10 gigatons (Gt = 10⁹ tons) of carbon dioxide to be removed from the atmosphere each year by the end of the century to achieve net carbon neutrality [1, 2]. The current supply of durable CDR—defined as carbon removal that is durable on timescales similar to or greater than the residence time of CO₂ in the atmosphere (~10² years)—is many orders of magnitude below this [3]. There is thus strong impetus for developing promising durable CDR approaches,

and significant amounts of private and public funding flowing into efforts to develop the basic science underlying durable CDR pathways and bring them to scale.

Enhanced weathering (EW) is one promising geochemical approach toward durable CDR [4–10]. This practice involves adding fine-grained cation-rich rock feedstocks (basalt, olivine, wollastonite, or steel slag) to soils, where they dissolve in the presence of elevated soil CO₂ to yield bicarbonate (HCO₃⁻). This bicarbonate can be transported by river/stream systems to the oceans, where much of it will remain stored on timescales on the order of 10⁴ years [9, 11, 12]. Carbonate (limestone) weathering—currently in widespread use as an agricultural practice for soil pH management—can also lead to alkalinity export and CDR. However, the dynamics of this process



are dependent in part on the pH at which weathering occurs, because bicarbonate produced from weathering reactions is unstable at relatively low soil pH [13, 14]. In any case, because EW has the potential to leverage extensive existing agricultural infrastructure, requires relatively little energy beyond that required to transport feedstock, and may have a range of agronomic and socioeconomic co-benefits, it has attracted considerable interest as a durable, cost-effective CDR pathway that has the potential to scale rapidly [5, 10, 15, 16].

However, there is a range of possible fates for cations released from EW feedstocks, including calcium carbonate or secondary clay mineral formation in terrestrial settings [17, 18], re-equilibration of the carbonic acid system in rivers and streams [8, 19, 20], and storage of cations on exchange sites within soils and in the lower critical zone [21–23]. In the case of secondary mineral formation, CO_2 can be permanently released back to the atmosphere, undoing the initial CDR. In the case of cation storage on exchange sites within soils CDR is instead delayed. In most instances cation sorption will drive conversion of HCO_3^- to CO_2 due to release of exchangeable acidity from the soil (figure 1), which is then rebalanced by HCO_3^- production once reversibly sorbed cations are released from the soil exchange complex when soils re-acidify.

Methods are currently being developed for tracking the initial release of cations from EW feedstocks [e.g. 24–26], and these approaches can provide an estimate of the ‘potential CDR’ at the initial point of feedstock dissolution. However, the timescales

over which this CDR potential will be realized are poorly known [16, 27]. This is critical for the technoeconomics of EW, because a ton of carbon removed immediately has more value than a ton of carbon removed in the future [e.g. 28–31]. As a result, offset purchase contracts using EW as a pathway should either accurately discount lagged carbon removal *ex-ante* or have *ex-post* guardrails for empirically verifying cation fluxes through the system over time. In either case, timescales of cation lag that are sufficiently long could potentially render project finance for EW deployments less favorable for conventional voluntary carbon markets.

Here, we use a reaction-transport code [32, 33] designed to simulate EW in managed lands to evaluate the throughput and storage timescales of anthropogenic alkalinity in agricultural soils. Through a series of idealized alkalinity flux simulations, we explore the main controls on cation storage and export from surface soils in key U.S. agricultural regions. We find that carbon removal lags induced by transient cation storage in soils can range from years to many decades—varying significantly across key agricultural regions of the U.S.—and suggest that carbon removal lags due to cation storage need to be considered in future EW research and deployment efforts. Lastly, we discuss the implications of these results for implementation of EW within carbon markets and suggest potential strategies through which background soil characteristics and deployment practice can both be leveraged to shorten carbon removal lags.

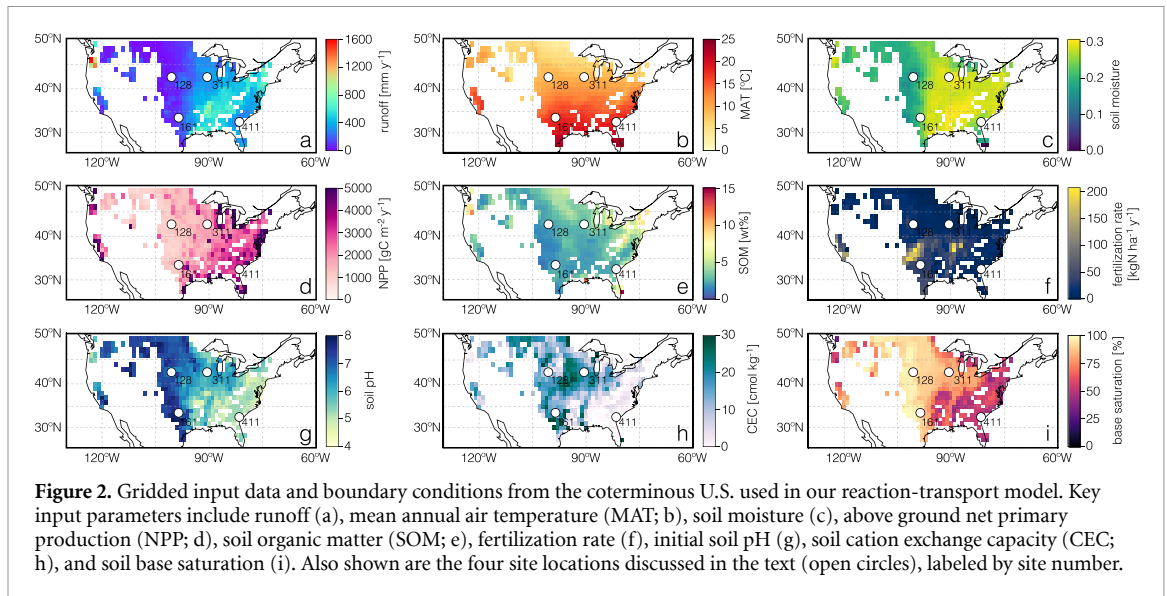


Figure 2. Gridded input data and boundary conditions from the coterminous U.S. used in our reaction-transport model. Key input parameters include runoff (a), mean annual air temperature (MAT; b), soil moisture (c), above ground net primary production (NPP; d), soil organic matter (SOM; e), fertilization rate (f), initial soil pH (g), soil cation exchange capacity (CEC; h), and soil base saturation (i). Also shown are the four site locations discussed in the text (open circles), labeled by site number.

2. Materials and methods

2.1. A gridded dataset for simulated alkalinity modification in U.S. agricultural regions

We focus here on key agricultural regions of the coterminous United States, basing our analysis on areas with a cropland fraction greater than 10% and gridded at a resolution of $1^\circ \times 1^\circ$. As boundary conditions for the initialization and spin-up of our reaction-transport code we use a series of gridded data products for runoff (defined as the sum of quick-flow runoff, recharge, and irrigation as in [34]), mean annual air temperature (MAT), soil moisture, aboveground net primary productivity (NPP), soil organic matter (SOM), fertilization rate, topsoil pH, soil cation exchange capacity (CEC), and soil base saturation (figure 2). All observational data are from the sources shown in table 1, and are either derived from the uppermost soil layer (0–20 or 30 cm, depending on the database) or averaged over the top 30 cm when depth-resolved at higher resolution. Data products are at a native resolution of $1^\circ \times 1^\circ$ or higher, with high-resolution data area-weighted and re-gridded to $1^\circ \times 1^\circ$. The partial pressure of CO_2 in the soil ($p\text{CO}_2$) was calculated as a function of net primary production (NPP) and temperature according to the method of Gwiazda and Broecker [35], as adapted and modified by Godd eris *et al* [36], Gaillardet *et al* [37], and Zeng *et al* [38].

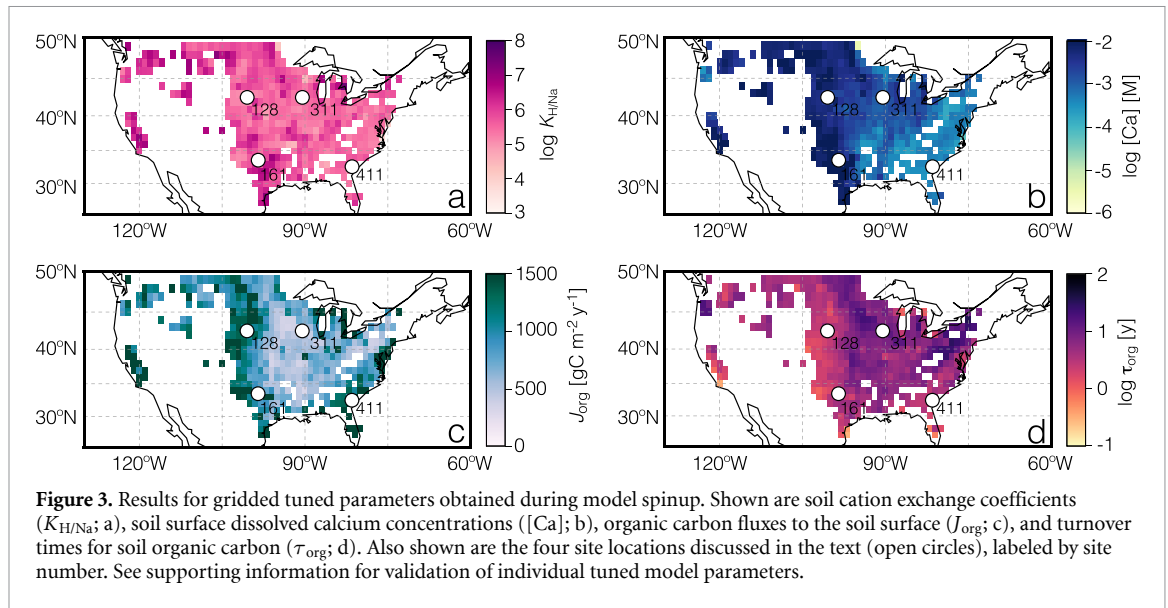
The reaction-transport model used here is designed to track feedstock-specific alkalinity release and cation/carbon biogeochemistry in managed soils [32, 33]. We adopt a model configuration that is essentially the same as that described in [32], which consists of two solid species (bulk soil phase plus SOM), one gaseous species (CO_2), and an inclusive range of aqueous species for evaluating charge balance and soil acid-base balance [33]. We use four

Table 1. Sources of observational data for model spin-up and tuning.

Parameter	Observational Dataset
Temperature	[39]
Soil moisture	[40]
Runoff/infiltration	[34]
Soil pH	[41]
Soil organic matter	[41]
Cation exchange capacity	[42]
Nitrification rate	[43]
Base saturation	[44]
Soil erosion	[45]
Soil porosity	[46]
Cropland fraction	[47]
Net primary production (NPP)	[48]

tuning parameters to initialize the soil column in each grid cell: (1) an aggregate cation exchange parameter ($K_{\text{H}/\text{Na}}$), which is then used to scale exchange parameters for all other cations; (2) a dissolved Ca^{2+} concentration at the upper boundary of the soil column, which essentially represents background carbonate weathering and historical agricultural liming; (3) an input flux of organic carbon (OC) to the soil; and (4) a time constant for OC turnover (figure 3). These parameters are tuned to match the observed values for soil pH, base saturation, SOM content, and estimated soil $p\text{CO}_2$ (figure 2), with the soil column in each grid cell being spun up for 10^5 years prior to alkalinity modification. Comparison of our baseline tuned parameter set (figure 3) with a range of observational data is provided in the supporting information.

Following spinup and initialization, we conduct alkalinity modification experiments in which an alkaline feedstock is added at a rate iteratively tuned to reach a specified agronomic target pH ($\text{pH}_t = 7.0$) at the end of each year for 100 years. We implement two



alkalinity sources—a default CaO feedstock, which is characterized by extremely rapid dissolution kinetics and simple cation stoichiometry, and an ‘instantaneous’ basalt feedstock, which has the stoichiometry of the idealized glassy basalt used by [32] but is specified to dissolve with the same speed as the CaO feedstock. This approach is designed to remove the time-dependent uncertainty in feedstock dissolution rates and to isolate the effects of cation exchange on the timescales of CDR. In the simulations shown here, feedstock is added continuously for each year and mixed homogeneously down to a depth of 25 cm. *In-silico* agronomic soil pH is calculated by the method described in [32]. The model domain for all simulations is 50 cm, which for our purposes is expected to yield a conservative (i.e., lower-bound) estimate of cation travel times through the soil column given that in the field cations will generally need to travel longer distances before being exported.

The boundary conditions of the reactive transport model are described in [33] and [32]. Briefly, the lower boundary is a parent rock composition for the solid phase and a zero-flux boundary for aqueous and gaseous phases with respect to diffusion/dispersion (zero concentration gradient). The upper boundary is a fixed composition for aqueous and gaseous species. The model allows for transport of solid, aqueous, and gaseous phases through advection and mixing, advection and diffusion/dispersion, and diffusion, respectively. Here, advection of solids and fluids is constrained respectively from USDA soil erosion rate data and runoff [34], while soil moisture impacts gaseous phase transport by modifying the soil tortuosity and diffusivity. The reaction kinetics are simulated for heterogeneous decomposition/formation of solid phases and redox reactions [33] and equilibrium is assumed for aqueous speciation and cation exchange [32, 33]. We also conduct control experiments branched from

the same initialization/spinup as that of the alkalinity modification experiments with identical boundary conditions other than the addition of alkaline feedstock.

2.2. CDR calculation methods

We evaluate CDR over time in the simulated soil column using three metrics, each of which is designed to correspond to a distinct set of techniques for measurement, reporting, and verification (MRV) of CDR in EW deployments. The first is scaled to the fraction of feedstock that dissolves in the soil (CDR_{diss}):

$$CDR_{diss} = \frac{\sum_{\theta} \gamma_{\theta} \Delta J_{\theta}^{diss}}{\sum_{\theta} \gamma_{\theta} \Delta J_{\theta}^{feed}} \quad (1)$$

where γ_{θ} is the molar ratio of potential CO_2 capture per unit dissolution of feedstock θ (e.g. $\gamma_{CaO} = 2$), J_{θ}^{feed} and J_{θ}^{diss} are deployment (spreading) and dissolution fluxes of feedstock θ ($\text{mol m}^{-2} \text{y}^{-1}$), respectively, and Δ denotes the flux difference between scenarios with and without feedstock deployment. Mechanistically, this metric corresponds to time-integrated solid-phase approaches for tracking on-field rates of CDR [4, 24, 25, 49, 50], which rely on measuring mobile cations and immobile elements in soil before and after feedstock application and using these measurements to estimate loss of base cations from applied feedstock.

The second CDR metric employed here is scaled to the reduction of gaseous CO_2 exchange between the soil column and the atmosphere (CDR_{diff}):

$$CDR_{diff} = \frac{\Delta J_{CO_2} - \Delta J_{SOC}}{\sum_{\theta} \gamma_{\theta} \Delta J_{\theta}^{feed}} \quad (2)$$

where γ_{θ} , J_{θ}^{feed} , and Δ are defined as above and J_{CO_2} and J_{SOC} are the soil-atmosphere flux of CO_2 ($\text{mol m}^{-2} \text{y}^{-1}$) and the decomposition flux ($\text{mol m}^{-2} \text{y}^{-1}$) of soil organic carbon (SOC),

respectively. Mechanistically, this metric reflects a decrease in the flux of CO_2 from the soil column to the atmosphere due to HCO_3^- production in the soil, and could in principle be measured through CO_2 gas fluxes from treated and control soils via eddy flux towers [51], flux chambers [52], or gas-phase CO_2 sensors [53]. In contrast to the solid-phase metric shown by equation (1), this metric tracks CDR directly and reflects additional HCO_3^- production (and a corresponding reduction of the soil-atmosphere CO_2 flux) due to soil management.

Lastly, we can scale CDR efficiency to the increase in advective fluxes of aqueous dissolved inorganic carbon species through the soil column (CDR_{adv}):

$$\text{CDR}_{\text{adv}} = \frac{\Delta J_{\text{DIC}} - \Delta J_{\text{SIC}}}{\sum_{\theta} \gamma_{\theta} \Delta J_{\theta}^{\text{feed}}} \quad (3)$$

where γ_{θ} , J_{θ}^{feed} , and Δ are defined as above and J_{SIC} and J_{DIC} represent the flux ($\text{mol m}^{-2} \text{y}^{-1}$) of soil inorganic carbon (i.e. mineral carbonates) dissolving into the soil system and total dissolved inorganic carbon (i.e. aqueous CO_2 , HCO_3^- , and CO_3^{2-}) advected out of soil column, respectively. Mechanistically, this metric reflects additional HCO_3^- production and advection out of the system due to feedstock application and could in principle be determined by an aqueous measurement at the field scale (e.g., alkalinity fluxes using a lysimeter [54]), point-collected dissolved solute measurements at the catchment scale [55], or possibly at larger scales through measurements of solute composition in stream/river systems [e.g. 13]. Similar to equation (2), this metric directly tracks net CDR in the soil column rather than gross alkalinity release.

Note that these metrics for CDR efficiency are referenced to the maximum potential CDR (e.g. $\sum_{\theta} \gamma_{\theta} \Delta J_{\theta}^{\text{feed}}$), which assumes that all base cations released from feedstock θ are leached immediately upon deployment and charge-balanced only by production of bicarbonate ions. At steady state, the reduction in soil-atmosphere CO_2 flux should be equivalent to the increase in bicarbonate advection ($\text{CDR}_{\text{diff}} \approx \text{CDR}_{\text{adv}}$). In the case of negligible cation sinks (e.g. secondary carbonate or silicate mineral phases) and on arbitrarily long timescales, $\text{CDR}_{\text{diss}} \approx \text{CDR}_{\text{diff}} \approx \text{CDR}_{\text{adv}}$. However, transient cation storage could result in lag periods for which CDR_{diff} (or $\text{CDR}_{\text{adv}} < \text{CDR}_{\text{diss}}$). This allows us to isolate and quantify cation storage lags through time-dependent offsets between CDR_{diss} and $\text{CDR}_{\text{diff}}/\text{CDR}_{\text{adv}}$.

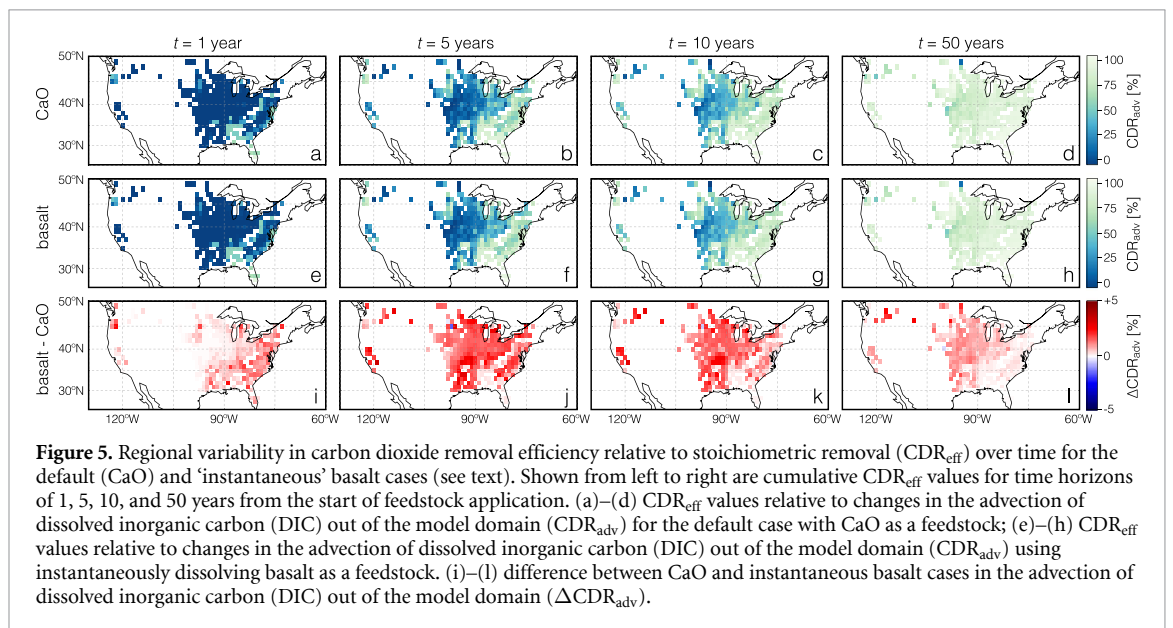
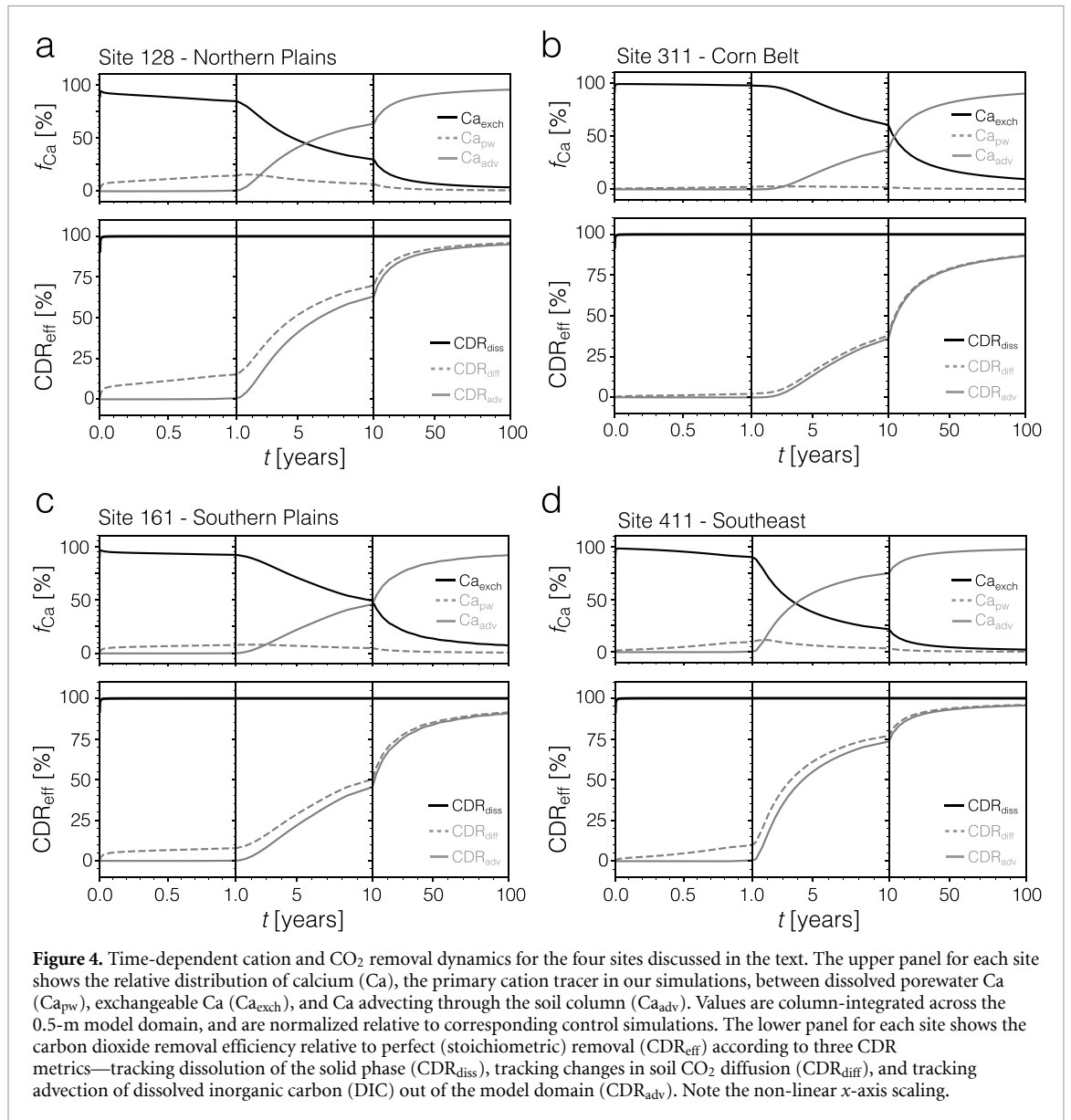
3. Results

We first examine timescales of alkalinity release, cation exchange, and carbon removal in four representative sites across key agricultural regions in the U.S.: (1) Site 128, located in the Northern Plains

region; (2) Site 311, located in the Corn Belt; (3) Site 161, located in the Southern Plains region; and (4) Site 411, located in the Southeast (figures 2 and 3). Alkalinity release into the system is specified to be effectively instantaneous across all sites (figure 4), with dissolution-based CDR (CDR_{diss}) matching effective CDR potential (CDR_{eff}) on a timescale of days to weeks. However, most of the alkalinity released from feedstock is initially stored as exchangeable calcium (Ca_{exch}) and is only gradually released back into the system as an advective cation flux (Ca_{adv}) over timescales ranging from years to decades (figure 4). This causes a significant lag in carbon removal relative to alkalinity input because it is only when the exchangeable calcium is released into the advective flux and charge balanced by HCO_3^- production that CDR can occur.

Although there is often a slight offset between carbon removal based on soil-atmosphere CO_2 exchange (CDR_{diff}) and advection of new DIC (CDR_{adv}) in the first decade, they track each other closely. However, actual carbon removal (tracked by both CDR_{diff} and CDR_{adv}) occurs over significantly longer timescales than those of alkalinity release (tracked by CDR_{diss} , here set to be effectively instantaneous) across all sites (figure 4). For example, for our deployment in the Corn Belt CDR_{diff} and CDR_{adv} reach less than 50% of the effective CDR potential after 10 years, with a timescale of over 50 years required to reach 80% of effective carbon removal (figure 4(b)). In contrast, realized CDR reaches nearly 80% of its potential within the first decade after deployment in the Southeast regional site (figure 4(d)).

Because the timescale required to achieve a particular CDR potential varies by region, we geospatially aggregate and weight carbon removal lags by overall alkalinity flux across key agricultural regions in the U.S. (figure 5). There are relatively few sites that show any tangible carbon removal in the first year despite instantaneous cation and alkalinity inputs, and these are generally restricted to scattered locations in the southeastern U.S. (Alabama, Georgia, and Florida; figures 5(a) and (e)). Many of the regions examined here show widespread areas that are below 50% of effective CDR potential after 5 year, and in some regions (the Corn Belt and Great Plains) it takes well over 10 years after instantaneous alkalinity input for carbon removal to occur locally (figures 5(d) and (h)). We find that instantaneous basalt simulations result in greater CDR at any given time, locally approaching nearly 10% of additional CDR capacity relative to the feedstock potential (figures 5(i)–(l)). This is due to the more complex cation stoichiometry of basalt, which in addition to Ca^{2+} contains a small amount of Na^+ that flushes through the system rapidly. This effect is most significant within the first ~ 5 year of simulated deployment in our



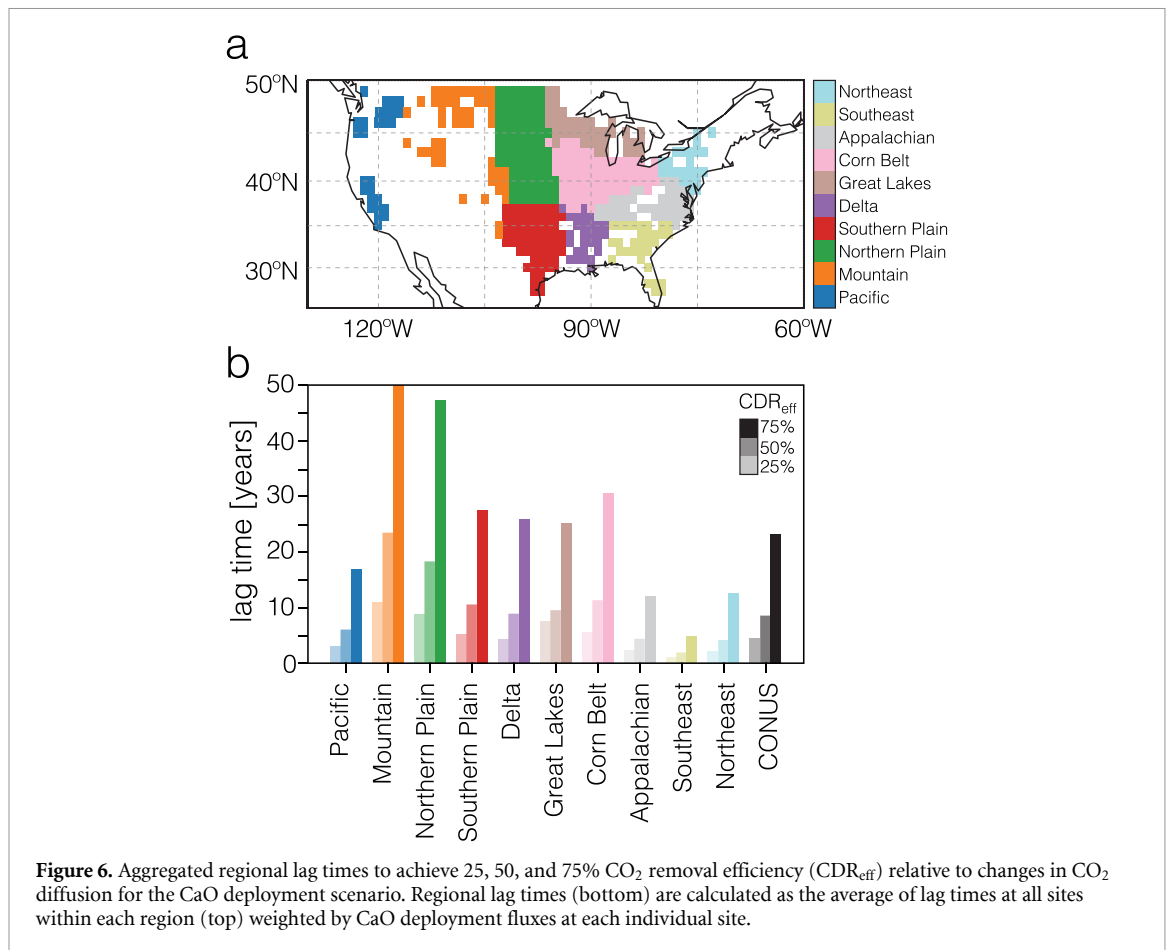


Figure 6. Aggregated regional lag times to achieve 25, 50, and 75% CO₂ removal efficiency (CDR_{eff}) relative to changes in CO₂ diffusion for the CaO deployment scenario. Regional lag times (bottom) are calculated as the average of lag times at all sites within each region (top) weighted by CaO deployment fluxes at each individual site.

model ensemble (figure 5(j)), but we would expect the overall magnitude and time dynamics of this effect to vary as a function of major cation chemistry of silicate feedstocks.

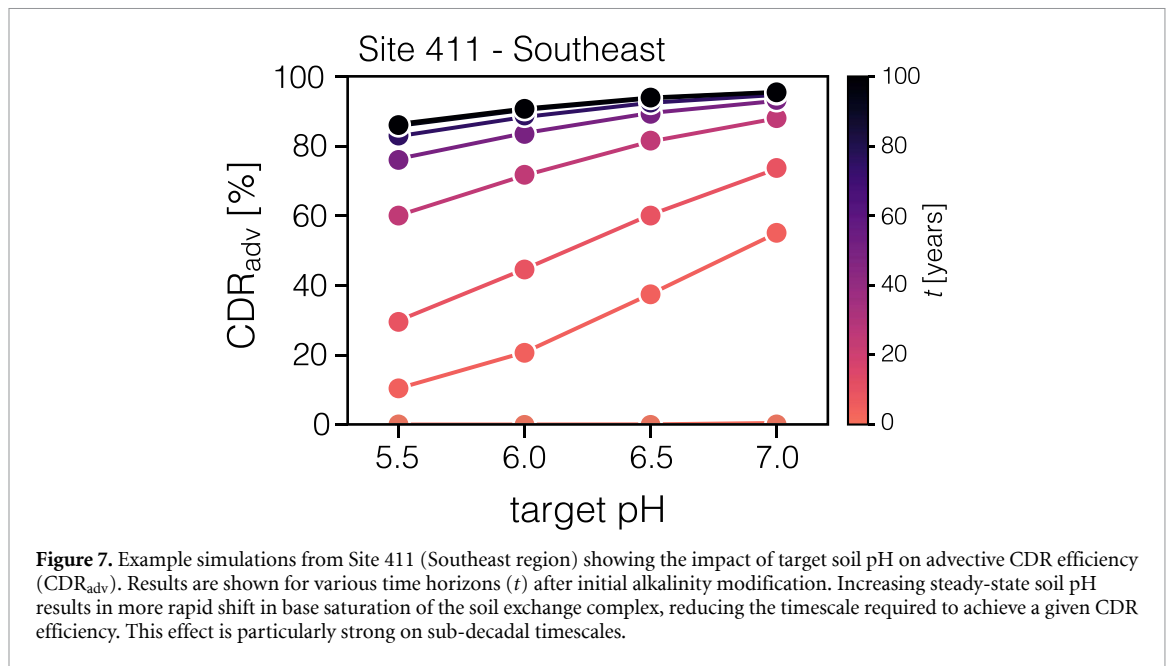
Although local CDR lags induced by cation storage can be high, in many cases regionally aggregated and flux-weighted CDR lags are much shorter. For instance, for key agricultural regions in the Midwest, Southeast, and Pacific regions flux-weighted CDR lags on achieving 50% CDR capacity are roughly 10, 3, and 7 years, respectively (figure 6). For CONUS croplands as a whole the flux-weighted lag times to achieve 25%, 50%, and 75% of CDR capacity are, respectively, 5, 8, and 22 years (figure 6). Lags on CDR induced by soil cation storage are thus expected to vary by orders of magnitude across scales, both at the field scale and when regionally aggregated, but in general our analysis suggests that over 50% of CDR capacity should be achievable within a decade of alkalinity release across all of the regions analyzed here.

The magnitude of cation lag should vary as a function of background soil characteristics. This is evident, for example, in the Southeast sites which, on average, show significantly shorter lag times overall because of very low CECs and high water fluxes (figures 2(h), 5(a),(e) and 6(b)). Cation lag times should also be impacted by soil management

practice—particularly the soil pH targeted for a given crop rotation or soil tilling style. For example, we find that higher target pH values can result in significantly higher CDR efficiency across the first few decades of increasing soil base saturation (figure 7) because of more rapid cation loading on the soil exchange complex. The impact of this can be significant—at Site 411, for instance, a target pH value of 5.5 results in an advective CDR efficiency of ~30% after ten years, while the same CDR efficiency can be achieved in only ~3 year at a target soil pH value of 7 (figure 7). The aggregate impacts of this will depend on the intersection between EW deployment strategy and agronomic practice, as target pH will depend on cash crop—many staple crops in the U.S. do well at soil pH values up to ~7, while some forage and specialty crops prefer more acidic pH [56].

4. Discussion

Our results suggest that CDR lags induced by cation exchange in agricultural soils can be significant, and in some cases can last multiple decades, adding to a robust evidence base for the following key conclusions: (1) cation sorption in soils with low base saturation (the ratio of cations to protons and aluminum in soil sorption sites) will delay climate-relevant CO₂



removal in EW deployments; (2) this lag time can be multiple years or even several decades locally; and (3) these lag times will vary geographically as a result of soil composition and climatology. Although we stress that although these basic conclusions are very likely robust, we do not currently have firm constraints on the uncertainty in lag times for any individual region or deployment protocol, and there is a pressing need to validate model estimates of carbon removal lag against real-world observations. As a result, we suggest that given the current state of knowledge reaction-transport models are not equipped to provide robust estimates of CDR lag for ready inclusion in carbon accounting schemes [e.g. 57].

One implication of the results presented here is that solid-phase tracers of cation release from EW feedstocks do not represent actual CDR at any time point, but rather a ‘potential’ CDR that may or may not be realized over a wide range of time horizons. Specifically, the condition that $CDR_{diss} \gg CDR_{adv}$ is ubiquitous spatially and persists for extended periods of time throughout the regions explored by our model ensemble. This supports a view articulated in previous attempts to use soil-based tracers of cation flux in the field that these tracers are tracking an idealized CDR potential rather than carbon removal itself [4, 24, 25]. Even if the idealized carbon removal potential of a particular feedstock is ultimately realized over a relatively short timescale, we argue that it is important to be as precise as possible when discussing the parameters that a given approach toward field-based MRV is tracking. This is particularly true for for-profit actors making compensatory claims on fossil fuel emissions.

There may be scope for optimizing the efficiency of alkalinity transport through soils via both deployment siting and land management practice.

For instance, continuously managing soil pH at a uniform optimal agronomic value is unlikely to be pursued in practice. Instead, pulsed alkalinity addition followed by cation flushing with strong acid from fertilizer application may increase the efficiency of alkalinity transport in managed soils. On the other hand, this approach may lead to lower time-integrated CDR overall. In addition, soil pH is a key driver of soil N_2O emissions through both direct impacts on microbial metabolism and ecosystem structure [58, 59] and through changes to crop nutrient use efficiency (NUE) [60–62]. As a result, intentional cation flushing could potentially increase time-integrated N_2O emissions, as this practice would be expected to result in extended periods of non-optimal soil pH for crop uptake and more acidic soil pH values overall, both of which could enhance soil N_2O emissions. Optimizing agricultural systems for overall mitigation of CO_2 -equivalent emissions (considering both CO_2 removal and N_2O emissions reduction) is an important topic for future work.

From a project siting perspective, regions with relatively low CEC values, large fluid infiltration rates, and increased pH and base cation abundance in the exchange complex at depth [e.g. 41], should all favor more rapid alkalinity export. Our simulations suggest that these conditions are particularly widespread in the Southeastern U.S. However, the tradeoffs between local/regional soil characteristics, optimal agronomic pH for a given local crop rotation, and the counteracting impacts of soil pH on the effectiveness of alkalinity export and initial feedstock dissolution are likely to be complex in practice. In addition, our simulation design intentionally neglects transient or permanent removal of base cations in deeper soils or during transport to the ocean in order to isolate the impacts of the soil exchange complex. Moving forward, there

is significant scope for end-to-end analysis of base cation transport efficiency including these additional impacts, and a pressing need for systematic model intercomparison and data-model validation.

An extended carbon removal lag after weathering induced by soil cation exchange has several significant implications for deployment of EW in a market framework. Most importantly, the economic value of carbon removal is time-varying, which means that EW deployments that aim to sell carbon offsets on a voluntary market should be able to accurately quantify the timing of climate-relevant CDR across timescales. One reasonable conclusion might be that suppliers of EW-based offsets on a voluntary market should be expected to either confront the technical challenge of quantifying carbon removal lags prior to deployment or the challenges to project finance associated with empirically verifying carbon removal over extended timescales prior to receiving revenue for offset production. Regardless, our results suggest that cation storage is ubiquitous, highly variable, and should be considered in EW deployments.

Perhaps most importantly, our results highlight the need for more empirical constraints on cation and alkalinity throughput in managed lands across scales. Accurate representation of the soil exchange complex in process-based models such as that explored here is challenging, and there is currently significant uncertainty in the dynamics of cation breakthrough in managed soils that are well out of steady state. Moving forward, the production of large datasets that can constrain cation fluxes and carbon removal lag times, some of which could be produced by private-sector suppliers of carbon removal through EW, would represent a major step forward in our ability to accurately quantify cation storage across a range of scenarios and deployment strategies. There is a pressing need for these data to be rigorously and transparently evaluated, and for the results to be leveraged in the development of process-based models of time-dependent soil cation exchange.

5. Conclusions

Soil biogeochemical modeling suggests that cation exchange dynamics in agricultural soils can lead to significant lags between alkalinity input from EW feedstocks and climate-relevant CDR. Lag times can vary locally from less than a year to many decades and will be controlled by background soil characteristics, land management practice, and land use history. In some cases, carbon removal lags can be reduced through thoughtful site selection and/or optimized soil pH management. However, carbon removal lags induced by soil cation storage should be ubiquitous in the field, and EW deployments that commodify carbon removal through charge balance must take storage-induced removal lags into account. In the near-term, this will require rigorous and

transparent validation of reaction-transport models against real-world observations of alkalinity throughput in managed lands.

Data availability statement

All data that support the findings of this study are included within the article (and any supplementary files). Data are available as of 06 June 2025, as follows.

Observational datasets used for model spin-up and tuning are: temperature [39], soil moisture [40], runoff/infiltration [34], soil pH [41], soil organic matter [41], cation exchange capacity [42], soil nitrification rate [43], base saturation [44], soil erosion rate [45], soil porosity [46], cropland fraction [47], net primary production [48]. The model code used here (SCEPTER-v1.0) is publicly available in [32].

Funding

CTR, NJP, and SZ acknowledge support from the U.S. Department of Energy, Office of Science Energy Earthshot Initiative. CTR and NJP acknowledge funding from the U.S. Department of Agriculture and the Grantham Foundation. NJP and TJS acknowledge funding from the Yale Center for Natural Carbon Capture (YCNCC). TJS acknowledges funding from the Swiss National Science Foundation (SNSF; P500PN_210790).

Author contributions

Conceptualization: YK, CTR, NJP.

Methodology: YK, SZ, CTR, NJP.

Investigation: YK, SZ, CTR, NJP.

Visualization: YK, CTR, NJP.

Funding acquisition: CTR, NJP.

Project administration: CTR, NJP.

Supervision: CTR, NJP.

Writing—original draft: CTR, YK.

Writing—review & editing: YK, CTR, NJP, SZ, JJ, TJS.

Conflict of interest


JJ is employed by Mati Carbon, A B-Corp owned by the not-for-profit organization Swaniti Initiative.

ORCID iDs

Y Kanzaki  <https://orcid.org/0000-0003-1400-1736>

N J Planavsky  <https://orcid.org/0000-0001-5849-8508>

S Zhang  <https://orcid.org/0000-0003-1745-4642>

T J Suhrhoff  <https://orcid.org/0000-0002-7934-7159>

C T Reinhard  <https://orcid.org/0000-0002-2632-1027>

References

- [1] IPCC 2018 *Global Warming of 1.5 °C An IPCC Special Report on the Impacts of Global Warming of 1.5 °C above Pre-industrial Levels and Related Global Greenhouse Gas Emission Pathways, in the Context of Strengthening the Global Response to the Threat of Climate Change, Sustainable Development, and Efforts to Eradicate Poverty* ed V Masson-Delmonte et al (Cambridge University Press) (<https://doi.org/10.1017/9781009157940>)
- [2] Rogelj J et al 2018 Scenarios toward limiting global mean temperature increase below 1.5 °C *Nat. Clim. Change* **8** 325–32
- [3] Smith S M et al 2024 The state of carbon dioxide removal—2nd edition (University of Oxford's Smith School of Enterprise and the Environment) (available at: <https://osf.io/f85qj/>)
- [4] Beerling D J et al 2024 Enhanced weathering in the US corn belt delivers carbon removal with agronomic benefits *Proc. Natl Acad. Sci.* **121** e2319436121
- [5] Beerling D J et al 2020 Potential for large-scale CO₂ removal via enhanced rock weathering with croplands *Nature* **583** 242–8
- [6] Kantzas E P et al 2022 Substantial carbon drawdown potential from enhanced rock weathering in the United Kingdom *Nat. Geosci.* **15** 382–9
- [7] Taylor L L, Quirk J, Thorley R M S, Kharecha P A, Hansen J, Ridgwell A, Lomas M R, Banwart S A and Beerling D J 2016 Enhanced weathering strategies for stabilizing climate and averting ocean acidification *Nat. Clim. Change* **6** 402–6
- [8] Zhang S, Planavsky N J, Katchinoff J, Raymond P A, Kanzaki Y, Reershemius T and Reinhard C T 2022 River chemistry constraints on the carbon capture potential of surficial enhanced rock weathering *Limnol. Oceanogr.* **67** S148–57
- [9] Kanzaki Y, Planavsky N J and Reinhard C T 2023 New estimates of the storage permanence and ocean co-benefits of enhanced rock weathering *PNAS Nexus* **2** pgad059
- [10] Baek S H, Kanzaki Y, Lora J M, Planavsky N, Reinhard C T and Zhang S 2023 Impact of climate on the global capacity for enhanced rock weathering on croplands *Earth's Future* **11** e2023EF003698
- [11] Renforth P and Henderson G 2017 Assessing ocean alkalinity for carbon sequestration *Rev. Geophys.* **55** 636–74
- [12] Lord N S, Ridgwell A, Thorne M C and Lunt D J 2015 An impulse response function for the “long tail” of excess atmospheric CO₂ in an earth system model *Glob. Biogeochem. Cycles* **30** 2–17
- [13] Oh N-H and Raymond P A 2006 Contribution of agricultural liming to riverine bicarbonate export and CO₂ sequestration in the Ohio River basin *Glob. Biogeochem. Cycles* **20** GB3012
- [14] Hamilton S K, Kurzman A L, Arango C, Jin L and Robertson G P 2007 Evidence for carbon sequestration by agricultural liming *Glob. Biogeochem. Cycles* **21** GB2021
- [15] Beerling D J et al 2018 Farming with crops and rocks to address global climate, food and soil security *Nat. Plants* **4** 138–47
- [16] Calabrese S, Wild B, Bertagni M B, Bourg I C, White C, Aburto F, Cipolla G, Noto L V and Porporato A 2022 Nano-to global-scale uncertainties in terrestrial enhanced weathering *Environ. Sci. Technol.* **56** 15261–72
- [17] Lal R 2007 Carbon management in agricultural soils *Mitig. Adapt. Strateg. Glob. Chang.* **12** 303–22
- [18] Bluth G J S and Kump L R 1994 Lithologic and climatologic controls of river chemistry *Geochim. Cosmochim. Acta* **58** 2341–59
- [19] Knapp W J and Tipper E T 2022 The efficacy of enhanced carbonate weathering for carbon dioxide sequestration *Front. clim.* **4** 928215
- [20] Harrington K J, Hilton R G and Henderson G 2023 Implications of the riverine response to enhanced weathering for CO₂ removal in the UK *Appl. Geochem.* **152** 105643
- [21] Spencer W F 1954 Influence of cation-exchange reactions on retention and availability of cations in sandy soils *Soil Sci.* **77** 129–36
- [22] Bolt G H, Bruggenwert M G M and Kamphorst A 1976 Adsorption of cations by soil *Developments in Soil Science (Soil Chemistry: A. Basic Elements vol 5)* ed G H Bolt and M G M Bruggenwert (Elsevier) pp 54–90
- [23] Appelo C A J 1994 Cation and proton exchange, pH variations, and carbonate reactions in a freshening aquifer *Water Resour. Res.* **30** 2793–805
- [24] Reershemius T et al 2023 Initial validation of a soil-based mass-balance approach for empirical monitoring of enhanced rock weathering rates *Environ. Sci. Technol.* **57** 19497–507
- [25] Suhrhoff T J, Reershemius T, Wang J, Jordan J S, Reinhard C T and Planavsky N J 2024 A tool for assessing the sensitivity of soil-based approaches for quantifying enhanced weathering: a US case study *Front. Clim.* **6** 1346117
- [26] Clarkson M O, Larkin C S, Swoboda P, Reershemius T, Suhrhoff T J, Maesano C N and Campbell J S 2024 A review of measurement for quantification of carbon dioxide removal by enhanced weathering in soil *Front. Clim.* **6** 1345224
- [27] Holden F J, Davies K, Bird M I, Hume R, Green H, Beerling D J and Nelson P N 2024 In-field carbon dioxide removal via weathering of crushed basalt applied to acidic tropical agricultural soil *Sci. Total Environ.* **955** 176568
- [28] Fearnside P M, Lashof D A and Moura-Costa P 2000 Accounting for time in mitigating global warming through land-use change and forestry *Mitig. Adapt. Strateg. Glob. Change* **5** 239–70
- [29] Richards K R 1997 The time value of carbon in bottom-up studies *Crit. Rev. Environ. Sci. Technol.* **27** S279–92
- [30] Groom B and Venmas F 2023 The social value of offsets *Nature* **619** 768–73
- [31] van Kooten G C, Withey P and Johnston C M T 2021 Climate urgency and the timing of carbon fluxes *Biomass Bioenergy* **151** 106162
- [32] Kanzaki Y et al 2024 *In-silico* calculation of soil pH by SCEPTER v1.0. *Geosci. Model Dev.* **17** 4515–32
- [33] Kanzaki Y, Zhang S, Planavsky N J and Reinhard C T 2022 Soil cycles of elements simulator for predicting TERrestrial regulation of greenhouse gases: SCEPTER v0.9 *Geosci. Model Dev.* **15** 4959–90
- [34] Reitz M, Sanford W E, Senay G B and Cazenais J 2017 Annual estimates of recharge, quick-flow runoff, and evapotranspiration for the contiguous US using empirical regression equations *J. Am. Water Res. Assoc.* **53** 961–83
- [35] Gwiazda R H and Broecker W S 1994 The separate and combined effects of temperature, soil pCO₂, and organic acidity on silicate weathering in the soil environment: formulation of a model and results *Glob. Biogeochem. Cycles* **8** 141–55
- [36] Goddérís Y, Williams J Z, Schott J, Pollard D and Brantley S L 2010 Time evolution of the mineralogical composition of Mississippi Valley loess over the last 10 kyr: climate and geochemical modeling *Geochim. Cosmochim. Acta* **74** 6357–74
- [37] Gaillardet J et al 1919 Global climate control on carbonate weathering intensity *Chem. Geol.* **527** 118762
- [38] Zeng S, Kaufmann G and Liu Z 2022 Natural and anthropogenic driving forces of carbonate weathering and the related carbon sink flux: a model comparison study at global scale *Glob. Biogeochem. Cycles* **36** e2021GB007096
- [39] Fick S E and Hijmans R J 2017 WorldClim 2: new 1km spatial resolution climate surfaces for global land areas *Int. J. Climatol.* **37** 4302–15
- [40] Wang Y, Mao J, Jin M, Hoffman F M, Shi X, Wullschlegel S D and Dai Y 2021 Development of observation-based global

- multilayer soil moisture products for 1970–2016 *Earth Syst. Sci. Data* **13** 4385–405
- [41] Poggio L, de Sousa L M, Batjes N H, Heuvelink G B M, Kempen B, Ribeiro E and Rossiter D 2021 SoilGrids 2.0: producing soil information for the globe with quantified spatial uncertainty *Soil* **7** 217–40
- [42] Liu S et al 2014 NACP MsTMIP: Unified North American Soil Map (ORNL DAAC) (<https://doi.org/10.3334/ORNLD AAC/1242>)
- [43] Pan B, Lam S K, Wang E, Mosier A and Chen D 2021 New approach for predicting nitrification and its fraction of N₂O emissions in global terrestrial ecosystems *Environ. Res. Lett.* **16** 034053
- [44] Batjes N H 2016 Harmonised soil property values for broad-scale modelling (WISE30sec) with estimates of global soil carbon stocks *Geoderma* **269** 61–68
- [45] USDA 2011 *RCA Appraisal 2011* (United States Department of Agriculture)
- [46] Rodell M et al 2004 The global land data assimilation system *Bull. Am. Meteorol. Soc.* **85** 381–94
- [47] Tuanmu M N and Jetz W 2014 A global 1-km consensus land-cover product for biodiversity and ecosystem modeling *Glob. Ecol. Biogeogr.* **23** 1031–45
- [48] Zhao M, Heinsch F A, Nemani R R and Running S W 2005 Improvements of the MODIS terrestrial gross and net primary production global data set *Remote Sens. Environ.* **95** 164–76
- [49] Kantola I B et al 2023 Improved net carbon budgets in the US Midwest through direct measured impacts of enhanced weathering *Glob. Change Biol.* **29** 7012–28
- [50] Reershemius T and Suhrhoff T J 2023 On error, uncertainty, and assumptions in calculating carbon dioxide removal rates by enhanced rock weathering in Kantola et al, 2023 *Glob. Change Biol.* **30** e17025
- [51] Baldocchi D D 2003 Assessing the eddy covariance technique for evaluating carbon dioxide exchange rates of ecosystems: past, present and future *Glob. Change Biol.* **9** 479–92
- [52] Pumpanen J et al 2004 Comparison of different chamber techniques for measuring soil CO₂ flux *Agric. For. Meteorol.* **123** 159–76
- [53] Yasuda Y, Ohtani Y, Mizoguchi Y, Nakamura T and Miyahara H 2007 Development of a CO₂ gas analyzer for monitoring soil CO₂ concentrations *J. For. Res.* **13** 320–5
- [54] Weihermüller L, Siemens J, Deurer M, Knoblauch S, Rupp H, Göttlein A and Pütz T 2007 *In situ* soil water extraction: a review *J. Environ. Qual.* **36** 1735–48
- [55] Larkin C S et al 2022 Quantification of CO₂ removal in a large-scale enhanced weathering field trial on an oil palm plantation in Sabah Malaysia. *Front. Clim.* **4** 959229
- [56] Service U.N.R.C. 2011 *National Agronomy Manual* (United States Department of Agriculture)
- [57] Balmford A, Keshav S, Venmans F, Coomes D, Groom B, Madhavapeddy A and Swinfield T 2023 Realizing the social value of impermanent carbon credits *Nat. Clim. Change* **13** 1172–8
- [58] Qiu Y et al 2024 Intermediate soil acidification induces highest nitrous oxide emissions *Nat. Commun.* **15** 2695
- [59] Hénault C et al 2019 Management of soil pH promotes nitrous oxide reduction and thus mitigates soil emissions of this greenhouse gas *Sci. Rep.* **9** 20182
- [60] Cui X, Bo Y, Adalibieke W, Winiwarter W, Zhang X, Davidson E A, Sun Z, Tian H, Smith P and Zhou F 2024 The global potential for mitigating nitrous oxide emissions from croplands *One Earth* **7** 401–20
- [61] Grados D, Butterbach-Bahl K, Chen J, Jan van Groenigen K, Olesen J E, Willem van Groenigen J and Abalos D 2022 Synthesizing the evidence of nitrous oxide mitigation practices in agroecosystems *Environ. Res. Lett.* **17** 114024
- [62] Lu C, Yu Z, Zhang J, Cao P, Tian H and Nevison C 2021 Century-long changes and drivers of soil nitrous oxide (N₂O) emissions across the contiguous United States *Glob. Change Biol.* **28** 2505–24